Research Article

Mathematical Methods in the Applied Sciences

Received 17 July 2013

Published online 28 November 2014 in Wiley Online Library

(wileyonlinelibrary.com) DOI: 10.1002/mma.3320
MOS subject classification: 65L07; 92B05; 92D30

Mathematical analysis of the transmission dynamics of brucellosis among bison

Emmanuel Abatih[a*†], Lenin Ron[b], Niko Speybroeck[a], Brian Williams[c] and Dirk Berkvens[a]

Communicated by G. Ding

In this study, a mathematical model previously proposed for the transmission dynamics of brucellosis among bison was mathematically analyzed. Our qualitative and quantitative findings support the general hypothesis that the infection will vanish from the herd when the basic reproduction number $R_0 < 1$ and will persist otherwise. A global sensitivity analysis was conducted, and the results of the Sobol indices indicated that the rate of loss of resistance (δ) and the recovery rate (v) were responsible for most of the variability in the expected number of infectious bison. On the other hand, according to the partial ranked correlation coefficients, the density-dependent reduction in birth (ϕ), the mortality rate (m), the transmission coefficient (β), and the recovery rate (v) exerted very high (and negative) correlations with the number of infectious bison, whereas the rate of loss of resistance (δ) and the calving rate (a) exerted very high (and positive) correlations with the number of infectious bison. Control measures should therefore aim at increasing the magnitude of ϕ, m, and v and reducing those of δ and a. In addition, experimental studies are needed to precisely estimate the rate of loss of resistance and the recovery rate in order to increase the accuracy of the expected number of infectious bison. Copyright © 2014 John Wiley & Sons, Ltd.

Keywords: bison; brucellosis; vaccination; population dynamics; sobol indices; direct transmission

1. Introduction

Brucellosis is a zoonotic bacterial infection capable of attacking multiple hosts. It is caused by bacteria of the genus *Brucella*, which manifests in different variants in different animal species. For example, *Brucella abortus* is mostly associated with cattle and bison and *Brucella melitensis* with sheep, goats, and humans [1, 2]. In animals, brucellosis is typically transmitted when susceptible animals come into direct contact with tissues or discharges from infectious animals, whereas in humans, common routes of infection include direct inoculation through cuts and abrasions in the skin or inhalation of infectious aerosols and ingestion of infectious unpasteurized milk or other dairy products. In animals, the infection localizes in the reproductive system and typically produces placentitis followed by abortion in the animal, usually during the last third of pregnancy, that is, between 5 and 7 months of gestation [1, 3]. It causes weight loss, abortion, and reduction in milk production in domestic livestock and undulant fever in humans [4–6]. Brucellosis infections may lead to serious economic consequences especially to the livestock production industries if no control measures are implemented. Even though brucellosis is essentiality a disease of domesticated livestock, its zoonotic potentials and the possibilities of inter-species transmission have made wildlife species an important source of or target for disease transmission.

The Yellowstone National Park (YNP), the first in the USA is one of the world's oldest and most famous. It is known for its wildlife and has many types of ecosystems with bison being the largest mammals. The identification of the first few cases of brucellosis in bison from the YNP dates back to 1917 using serological tests from two bison, which had been aborted [7]. Following this, brucellosis surveillance in the YNP has been characterized by opportunistic testing, and only occasionally has systematical testing been done [4]. Brucellosis has been virtually eliminated in domestic livestock in the USA after decades of expensive governmental disease prevention, control, and eradication programs. The most likely source of transmission of brucellosis to humans and the risk of reintroduction of

[a] *Unit of Epidemiology, Department of Biomedical Sciences, Institute of Tropical Medicine, Nationalestraat 155,2000 Antwerp, Belgium*
[b] *Centro Internacional de Zoonosis (CIZ), P.O. Box: 17-03-100, Geronimo Leyton SN, y Gato Sobral, Ciudadela Universitaria, Quito, Ecuador*
[c] *South African Centre for Epidemiological Modeling and Analysis (SACEMA), Stellenbosch, South Africa*
* *Correspondence to: Emmanuel Abatih, Unit of Epidemiology, Department of Biomedical Sciences, Institute of Tropical Medicine, Nationalestraat 155,2000 Antwerpen, Belgium.*
† *E-mail: enjiabatih@itg.be*

brucellosis into livestock is from infected populations of free-ranging bison [8]. The risk of transmission of brucellosis from bison to cattle and other livestock species is an issue that is under hot debate. It is obvious that without informed management actions, the bison population will continue to grow and may expand beyond the carrying capacity of the YNP [9]. Consequently, culling has been periodically executed as a population control measure [5].

Even though brucellosis in bison in the YNP poses a significant treat to the cattle industry following the risk of its transmission from bison to cattle, mathematical models that characterize the dynamics, determine thresholds for transmission and persistence, and that can provide a platform for evaluating the effects of control policies such as vaccination and culling have been rarely investigated in detail. In the wake of the recent controversial ethical and ecological debates following the culling of bison in the YNP, there is a need for a modelling framework based on the current knowledge of the epidemiology of brucellosis among bison. This article is based on the paper by [4] where a mathematical model for studying the epidemiology of brucellosis among bison in the YNP was established [4]. Their model characterized the epidemiology of brucellosis in the YNP, albeit the transmission of dynamics was not explored in detail. In addition, the influence of uncertainties around parameter values on the estimated outputs was not investigated.

The aim of this paper was therefore to determine thresholds, equilibria, and their stability for the systems of ordinary differential equations that describe the transmission dynamics of brucellosis in bison. In addition, a theoretical framework was provided for evaluating the effects of brucellosis control programs such as culling and vaccination, and a global sensitivity analysis was conducted to determine parameter values for which the level of uncertainty has to be decreased in order to reduce the uncertainties in output parameters [10] and also provide information that can be used to inform decision makers on which parameters to target in order to achieve desired levels of prevention and control.

The paper is structured as follows. The simplifying assumptions used in the model building process are stated in Section 2. The model is then developed based on the stated assumptions and on the paper by Dobson and Meagher (1996). This section also discusses threshold parameters. Transmission dynamics of brucellosis in bison was characterized by studying the local and global stability properties of steady-state solutions of the system as discussed in Section 3. Section 4 discusses the results of numerical simulations demonstrating steady states and the influence of control policies such as culling and vaccination. This section ends with a discussion of the results of the global sensitivity analysis. A discussion of the main findings and some future perspectives is presented in Section 5.

2. Model formulation

2.1. *Assumptions*

The transmission dynamics of brucellosis is complex, therefore, several assumptions were made to facilitate the understanding of its transmission dynamics in a typical bison herd. The implications of relaxing one or more of these assumptions will be discussed.

- The herd consists of a total of N individuals each of the three states at any give time t
  - The susceptible class, S
  - The infectious class, I and
  - The recovered class, R
- Transmission is via direct contact among bison and also vertically from bison to their calves.
- The life span of a bison is between 20 and 25 years [11].
- Transmission is independent of seasonal fluctuations

The dynamics are constructed over a study period of 50 years with yearly time steps. In the model developed by Dobson and Meagher (1996), it was assumed that brucellosis increases mortality (mostly among calves) so both demography and epidemiology were incorporated into the equations that characterize the population dynamics of brucellosis. For example, a consequence of the infectiousness of the disease is that the fertility of the female bison will be reduced. Applying the aforementioned assumptions, using the parameters in Table I and the flow diagram in Figure 1, the following model consisting of a set of coupled differential equations is considered [4]:

$$\begin{aligned}
\frac{dS(t)}{dt} &= (a-\phi N)[S+R+I\rho(1-e)] - mS + \delta R - \beta\frac{I}{N}S \\
\frac{dI(t)}{dt} &= \beta\frac{I}{N}S + e\rho(a-\phi N)I - (\alpha+m+v)I \\
\frac{dR(t)}{dt} &= vI - (m+\delta)R \\
\frac{dN(t)}{dt} &= (a-\phi N)N - (a-\phi N)(1-\rho)I - \alpha I - mN \\
& S(0) > 0,\ I(0) \geq 0,\ R(0) \geq 0 \text{ and } N(0) > 0
\end{aligned} \tag{1}$$

Table I. Variables and parameter definition for System (1).	
S	Susceptible bison population (*heads*)
I	Infectious bison population (*heads*)
R	Recovered bison population (*heads*)
N	Time varying total population (*heads*)
ϕ	Density dependent reduction in births ($heads^{-1}year^{-1}$)
ρ	Reduction of fecundity in infectious bison (unit-less)
α	Disease related death rate ($year^{-1}$)
β	Transmission coefficient ($year^{-1}$)
δ	Rate of lost of resistance ($year^{-1}$)
e	Proportion of vertical transmission (unit-less)
v	Recovery rate ($year^{-1}$)
m	Per capita disease free death rate ($year^{-1}$)
a	Birth rate ($year^{-1}$)

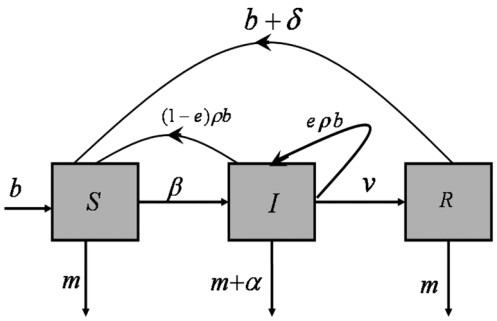

Figure 1. Schematics of the dynamics of brucellosis in a bison herd over a 50-year period. The flow diagram represents the various states with susceptible bison represented by *S*, infectious bison by *I*, and those that have recovered by *R*. The flow from one class to another is indicated with arrows, and the parameters are explained in Table I with $b = (a - \phi N)$.

All the parameters α, β, m, ϕ, ρ, and δ are assumed to be positive constants. The first equation in System 1 describes the dynamics of the susceptible bison population (S). Bison enter the susceptible class through birth from the susceptible and recovered classes at the net per capita birth rate of $(a - \phi N)$ and from the infectious class at the overall per capita birth rate of $\rho(1 - e)(a - \phi N)$. The parameter, ϕ, represents the density-dependent reduction in host births. This class is also augmented through lost of immunity by bison already in the recovered class at the per capita rate of δ. The susceptible bison population is reduced through natural mortality at the per capita rate of m and through infections following contact with infectious bison. Susceptible bison enter the infectious class at a per capita rate of $\frac{\beta I}{N}$, with β denoting the transmission coefficient and given by the contact rate multiplied by the probability of infection per contact with a susceptible and $\frac{I}{N}$, the fraction of infectious bison (also known as frequency-dependent transmission). It is worth noting that the infectious bison have a reduced birth rate modelled by ρe, where e is the proportion of infected calves, and ρ is the reduction in fertility due to the infection. In addition, because it was assumed in the model by [4] that brucellosis is vertically transmitted and that the infected newborns reside in the infectious class, the vertical transmission was modelled through the term $e\rho(a - \phi N)$ [4]. The infectious population is reduced through natural mortality at the per capita rate of m and also through recovery from the infection at a recovery rate of v.

3. Model analysis

3.1. *Boundedness of System (1)*

The boundedness of the solutions of System (1) guarantees its mathematical and epidemiological validity [12]. In addition, it is necessary to determine the persistence of steady states of the system. To show that System (1) is bounded, it suffices to show that the region

$$\Omega = \{(S, I, R : S > 0,\ I \geq 0,\ R \geq 0,\ and\ S + I + R \leq N\}$$

is positive invariant. In other words, it suffices to show that all trajectories that have their initial values in Ω remain in Ω for all positive time. Summing up the first three equations of (1), using basic comparison theorems ($\rho I < I$ because $\rho < 1$ and $(a - \phi N)[S + I + R] \leq (a - \phi N)N) - m * N$ and the constraint that $S + I + R = N$, we have

$$N'(t) = (S(t) + I(t) + R(t))' = (a - \phi N)[S + \rho I + R] - mN \leq (a - \phi N)N - mN$$

It immediately follows by solving the differential inequality that

$$N(t) \leq \frac{(a-m)N(0)e^{(a-m)t}}{\phi N(0)(e^{(a-m)t}-1)+(a-m)}$$

Therefore, because $\lim_{t\to\infty} \frac{(a-m)}{\phi\left(1-\frac{1}{e^{(a-m)t}}\right)+\frac{(a-m)}{e^{(a-m)t}}} = \frac{(a-m)}{\phi}$, all solutions of System (1) in finite time must satisfy $S+I+R \leq \frac{(a-m)}{\phi}$.

All analysis of System (1) will therefore be limited to the region Ω given by

$$\Omega = \left\{(S,I,R) : S>0, I \geq 0, R \geq 0, \text{ and } S+I+R \leq \frac{(a-m)}{\phi}\right\}$$

Therefore, System (1) is mathematically and epidemiologically well posed.

3.2. *Threshold parameters*

In the absence of the disease, the rate of change of the population size can be expressed as follows:

$$\frac{dN(t)}{dt} = (a-\phi N)N - mN$$

Using partial fractions and solving the numerical expression, the following solution was obtained:

$$N(t) = \frac{aN(0)e^{(a-m)t}}{\phi N(0)(e^{(a-m)t}-1)+(a-m)}$$

It follows that $\lim_{t\to\infty} N(t) = \lim_{t\to\infty} \frac{(a-m)}{\phi\left(1-\frac{1}{e^{(a-m)t}}\right)+\frac{(a-m)}{N(0)e^{(a-m)t}}} = \frac{(a-m)}{\phi}$

The transmission dynamics of brucellosis in the YNP is governed by the basic reproduction number R_0, which is defined as the expected number of secondary infected bison resulting from the introduction of one infectious bison in an entirely susceptible bison population. It is given by the product of the rate at which newly infected bison arise and the natural and disease death-adjusted average infectious period [13].

For System (1), (R_0) was simply derived by considering that for the infection to be established in the bison population, $\frac{dI}{dt} > 0$. This leads to the following inequalities:

$$\beta\frac{I}{N}S + e\rho(a-\phi N)I - (\alpha+m+v)I > 0$$

or

$$\beta\frac{S}{S+I+R} + e\rho(a-\phi(S+I+R)) - (\alpha+m+v) > 0$$

but for an infection free herd, $I=0$, $R=0$, and $S=\frac{a-m}{\phi}$, therefore,

$$\beta + e\rho(a-(a-m)-(\alpha+m+v)) > 0$$

from which it follows that $\beta + e\rho m - (\alpha+m+v) > 0$ or $\frac{\beta+e\rho m}{(\alpha+m+v)} > 1$

The basic reproduction number is thus given by $R_0 = \frac{\beta+e\rho m}{(\alpha+m+v)}$.

3.3. *Rest points and their stability*

3.3.1. Infection free steady state. The potential rest points for System (1) are obtained by setting the right-hand side of the first three equations to zero. The following infection free steady state given by $E_0 = \left(\frac{a-m}{\phi}, 0, 0\right)$ exists for all parameter values satisfying the condition that $a > m$ and $\phi > 0$.

The local asymptotic stability of $E_0 = \left(\frac{a-m}{\phi}, 0, 0\right)$ is determined by the signs of the eigen values of the Jacobian matrix obtained by linearizing System (1) around E_0. The Jacobian represents the best linear approximation of System (1) at E_0 and is given by

$$\mathbf{J}(E_0) = \begin{pmatrix} m_{11} & m_{12} & m_{13} \\ 0 & m_{22} & 0 \\ 0 & m_{32} & m_{33} \end{pmatrix}$$

where

$$m_{11} = -(a-m), m_{12} = m\rho(1-e) - (a-m) - \beta, m_{13} = \delta - a + 2m$$
$$m_{22} = \beta + e\rho m - (\alpha + m + v), \quad m_{32} = v \text{ and } m_{33} = -(m+\delta)$$

The eigen values of $\mathbf{J}(E_0)$ satisfy $det(\mathbf{J}(E_0) - \lambda\mathbf{I}) = 0$, which leads to the following characteristic equation:

$$(m_{11} - \lambda)(m_{22} - \lambda)(m_{33} - \lambda) = 0$$

This yields the following eigen values:

$$\lambda_1 = m_{11}, \quad \lambda_2 = m_{22} \text{ and } \lambda_3 = m_{33}$$

E_0 is locally asymptotically stable if and only if all the eigen values are negative.

$\lambda_1 < 0 \Rightarrow -(a-m) < 0$, from which it follows that $\lambda_1 < 0$ iff $a > m$.
$\lambda_2 < 0$ iff $\frac{\beta + e\rho m}{(\alpha+m+v)} < 1$ or $R_0 < 1$.
$\lambda_3 < 0$ by observation.

Therefore, E_0 is locally asymptotically stable iff $R_0 < 1$ and $a > m$.

The global stability of the infection-free steady state, E_0, is established in the following proposition:

Proposition 1.1
All solutions in the region Ω approach the infection-free equilibrium E_0 for $R_0 \leq 1$.

Proof
Consider the Lyapunov function: $W : \Omega \to R$, $W = \frac{[(S-S_0)+I+R]^2}{2} + \frac{(1-\rho)I^2}{2e\rho} + \frac{(\alpha+2m)R^2}{2v}$, which is well-defined and continuous in Ω. W=0 at $(S, I, R) = \left(\frac{a-m}{\phi}, 0, 0\right)$ and positive if $(S, I, R) \neq \left(\frac{a-m}{\phi}, 0, 0\right)$. Also, for any solution $\phi(t)$, $W(\phi(t_0)) \geq W(\phi(t_1))$ for $t_1 > t_0$, where $\phi(t_j) \in W((S_0, I_0, R_0)) \setminus (s_0, i_0, r_0)$. The Lyapunov derivative of W is given by

$$\dot{W} = [(S-S_0) + I + R][S' + I' + R'] + \frac{(1-\rho)II'}{e\rho} + \frac{\alpha RR'}{v}$$

which expands to

$$\dot{W} = [(S-S_0) + I + R][(a-\phi N)N - (a-\phi N)(1-\rho)I - \alpha I - mN] + \left[\frac{(1-\rho)}{e\rho}\right]\left[\frac{\beta I^2 S}{N} + e\rho(a-\phi N)I^2 - (\alpha+m+v)I^2\right] + \left[\alpha IR - \frac{(m+\delta)}{v}R^2\right]$$

Substituting $a = \phi S_0 + m$, we have that

$$\dot{W} = [(S-S_0) + I + R][(-\phi N((S-S_0) + I + R) + \phi(1-\rho)I((S-S_0) + I + R) - mI(1-\phi) - \alpha I] + \frac{(1-\rho)I^2 S}{e\rho N} - \phi(S-S_0)(1-\rho)I^2 + m(1-\rho)I^2 - \phi(1-\rho)(I+R)I^2 - \frac{(\alpha+m+v)(1-\rho)I^2}{e\rho} + [\alpha IR - \frac{\alpha(m+\delta)}{v}R^2]$$

which simplifies to

$$\dot{W} = -[(S-S_0) + I + R]^2[\phi(S+R) + \phi\rho I] - \phi I(I+R) - \phi(S-S_0) - m(S-S_0)I(1-\rho) - m(I+R)I(1-\rho) + \frac{(1-\rho)I^2 S}{e\rho N} - \phi(S-S_0)(1-\rho)I^2 + m(1-\rho)I^2 - \phi(1-\rho)(I+R)I^2 - \frac{(\alpha+m+v)(1-\rho)I^2}{e\rho} + \left[\alpha IR - \frac{\alpha(m+\delta)}{v}R^2\right]$$

Further simplification yields that

$$\dot{W} = -[(S-S_0) + I + R]^2[\phi(S+R) + \phi\rho I] - (S-S_0)I[\alpha + m(1-\rho)] - mIR(1-\rho) - I^2[\alpha + \phi(S-S_0)(1-\rho) + \phi(1-\rho)(I+R)] - \frac{\alpha(m+\delta)}{v}R^2 - \frac{(1-\rho)I^2}{e\rho N}[(\alpha+m+v)N - \beta S]$$

Adding and subtracting $\frac{e\rho mS(1-\rho)I^2}{e\rho N}$ to the right-hand side and writing in terms of R_0, it follows that

$$\dot{W} = -[(S-S_0) + I + R]^2[\phi(S+R) + \phi\rho I] - (S-S_0)I[\alpha + m(1-\rho)] - mIR(1-\rho) - I^2[\alpha + \phi(S-S_0)(1-\rho) + \phi(1-\rho)(I+R)] - \frac{\alpha(m+\delta)}{v}R^2 - \frac{(1-\rho)I^2 S}{e\rho N}\left[\frac{(\alpha+m+v)(I+R)}{S} + (\alpha+m+v)(1-R_0)\right] - \frac{e\rho mS(1-\rho)I^2}{e\rho N}$$

If $R_0 \leq 1$, then $\dot{W} \leq 0$. In addition, we note that $\dot{W} = 0$ iff $S = S_0$, $I = 0$, and $R = 0$.

Therefore, the largest compact invariant set in $\{(S, I, R) \in \Omega : \dot{W} = 0\}$ is the singleton $\{E_0\}$, where E_0 is the disease-free equilibrium. It thus follows from the Lyapunov–Lasalle [14] theorem that E_0 is globally asymptotically stable in Ω and so every trajectory of System (1) approaches the infection-free equilibrium for $R_0 \leq 1$. E_0 is the unique steady state for System (1) when $R_0 \leq 1$. □

3.3.2. Endemic steady state. When the infection-free steady state is locally or globally asymptotically unstable, the system may settle at an endemic equilibrium. For System (1), the endemic equilibrium is given by $E_e = (S_e, I_e, R_e)$, where S_e, I_e, and R_e were obtained as follows: from the second equation of (1), it follows that

$$0 = \frac{\beta}{N}S + e\rho(a - \phi N) - (\alpha + m + v) \text{ or } S_e = \frac{N_e}{\beta}[(\alpha + m + v) + e\rho(\phi N_e - a)]$$

Next, from the third equation of System (1), we have that $R_e = \frac{vI_e}{(m+\delta)}$.

Using the equality, $N_e = S_e + I_e + R_e$ and substituting the expression for S_e, I_e, and R_e, we have that

$$I_e = \frac{N_e(m + \delta)}{\beta(m + \delta + v)}[\beta - (\alpha + m + v) - e\rho\phi N_e + e\rho a]$$

To derive conditions for the existence of the endemic equilibrium, we start by observing that

- $S_e > 0$ iff $N_e > \frac{a}{\phi}$.
- $I_e > 0$ iff $\beta > (\alpha + m + v) + e\rho\phi N_e - e\rho a$ from which it follows that $R_0 > 1$.

It therefore follows that E_e exists iff $N_e > \frac{a}{\phi}$ and $R_0 > 1$.
The local and global asymptotic stability of this endemic rest point is given as follows:
For E_e, the variational (stability) matrix of System (1) is given by

$$\mathbf{J}(E_e) = \begin{pmatrix} m_{11} & m_{12} & m_{13} \\ m_{21} & m_{22} & m_{23} \\ 0 & v & m_{33} \end{pmatrix}$$

where $m_{11} = -\left[\phi(S_e + R_e + I_e\rho(1-e)) + (\phi N_e - a) + m + \frac{\beta I_e(I_e+R_e)}{N_e^2}\right]$, $m_{12} = -\left[\phi(S_e + R_e + I_e\rho(1-e)) + \rho(1-e)(\phi N_e - a) + \frac{\beta S_e(S_e+R_e)}{N_e^2}\right]$, $m_{13} = \phi\,[N_e + R_e] - \phi\,[S_e + I_e\phi(1-e)] + (a + \delta) + \frac{\beta S_e I_e}{N_e^2}$, $m_{21} = \frac{I_e(\alpha+m+v)}{N_e}\left[R_0 - 1 + \frac{e\rho(a-m)}{\alpha+m+v}\right]$, $m_{22} = -\left[\frac{\beta S_e I_e}{N_e} + e\rho I_e\right]$, $m_{23} = -I_e\left[\frac{\beta S_e I_e}{N_e} + e\rho\phi\right]$, $m_{33} = -(\delta + m)$

The eigen values of $\mathbf{J}(E_e)$ satisfy: $det(\mathbf{J}(E_e) - \epsilon\mathbf{I}) = 0$, from which the following characteristic equation is obtained:

$$0 = \epsilon^3 + A_1\epsilon^2 + A_2\epsilon + A_3$$

where

- $A_1 = -m_{11} - m_{22} - m_{33}$
- $A_2 = m_{11}m_{33} + m_{11}m_{22} + m_{22}m_{33} - m_{12}m_{21} - vm_{23}$ and
- $A_3 = m_{12}m_{21}m_{33} - m_{11}m_{22}m_{33} - vm_{13}m_{21} + vm_{11}m_{23}$

According to the Routh–Hurwitz criterion [15], E_e is locally asymptotically stable iff the following three conditions hold:

1. $A_1 > 0$
2. $A_3 > 0$ and
3. $A_1A_2 > A_3$

- For A_1,
  - $m_{11} < 0$ iff $N_e > \frac{a}{\phi}$
  - $m_{22} < 0$ iff $N_e > \frac{a}{\phi}$ and $R_0 > 1$
  - $m_{33} < 0$

  Therefore $A_1 > 0$ iff $N_e > \frac{a}{\phi}$ and $R_0 > 1$
- For A_3,
  - $vm_{11}m_{23} > 0$ because $m_{11} < 0$ and $m_{23} < 0$

- $m_{12}m_{21}m_{33} > 0$ iff $N_e > \frac{a}{\phi}$ and $R_0 > 1$ because $m_{12} < 0, m_{21} > 0$, and $m_{33} < 0$
- $-m_{11}m_{22}m_{33} > 0$ because $m_{11} < 0, m_{22} < 0$ and $m_{33} < 0$
- $-vm_{13}m_{21} > 0$ because $m_{21} > 0$ and $m_{13} < 0$ ($m_{13} < 0$ iff $R_0 > 1$)

- For $A_1A_2 - A_3 = m_{11}m_{12}m_{21} - m_{11}^2m_{22} + m_{12}m_{21}m_{22} - m_{11}m_{22}^2 - m_{11}^2m_{33} - 2m_{11}m_{22}m_{33} - m_{22}^2m_{33} - m_{11}m_{33}^2 - m_{22}m_{33}^2 + m_{22}m_{23}v + m_{23}m_{33}v + m_{13}m_{21}v$

  - $vm_{33}m_{23} > 0$ because $m_{33} < 0$ and $m_{23} < 0$
  - $m_{22}m_{23}v > 0$ because $m_{22} < 0$ and $m_{23} < 0$
  - $m_{11}m_{12}m_{21}$ because $m_{11} < 0, m_{12} < 0$, and $m_{21} > 0$
  - $-m_{11}^2m_{22} > 0$ and $-m_{22}m_{33}^2$ because $m_{22} < 0$
  - $m_{12}m_{21}m_{22} > 0$ because $m_{22} < 0, m_{12} < 0$, and $m_{21} > 0$
  - $-m_{11}m_{22}^2$ and $-m_{11}m_{33}^2$ because $m_{11} < 0$
  - $-m_{11}^2m_{33} > 0$ and $-m_{22}^2m_{33}$ because $m_{33} < 0$
  - $-2m_{11}m_{22}m_{33} > 0$ because $m_{11} < 0, m_{22} < 0$, and $m_{33} < 0$
  - $m_{13}m_{21}v < 0$ because $m_{13} < 0$ and $m_{21} > 0$.

  The term $m_{13}m_{21}v$ was therefore combined with other terms such as $m_{11}m_{12}m_{21}$ and $m_{12}m_{21}m_{22}$. The combined expression was expanded out using the Expand[] function in Mathematica into 96 terms, 41 of which were negative. Pairing negative and positive terms in this expression yielded a positive combined expression iff $R_0 > 1$ and $N_e > \frac{a}{\phi}$.

It was therefore concluded that the endemic steady state E_e is locally asymptotically stable provided that $R_0 > 1$ and $N_e > \frac{a}{\phi}$. The global stability of the endemic steady state E_e is established in the following proposition:

Proposition 1.2
All solutions in the region Ω approach the infection-free equilibrium E_e for $R_0 \geq 1$.

Proof
Consider the Lyapunov function: $V : \Omega \to R, V = \frac{[(S-S_e)+(I-I_e)+(R-R_e)]^2}{2} + \frac{(1-\rho)}{e\rho}\left[I - I_e - I_e * ln\left(\frac{I}{I_e}\right)\right] + \frac{\alpha(R-R_e)^2}{2v}$

which is well-defined and continuous in Ω. V=0 at $(S, I, R) = (S_e, I_e, R_e)$ and positive if $(S, I, R) \neq (S_e, I_e, R_e)$. Also for any solution $\phi(t)$, $V(\phi(t_0)) \geq V(\phi(t_1))$ for $t_1 > t_0$, where $\phi(t_j) \in V((S_e, I_e, R_e)) \setminus (s_e, i_e, r_e)$. The Lyapunov derivative of V is given by $\dot{V} = [(S - S_e) + (I - I_e) + (R - R_e)][S' + I' + R'] + \frac{(1-\rho)}{e\rho}\left[\frac{(I-I_e)I'}{I}\right] + \frac{\alpha(R-R_e)R'}{v}$, which expands to

$$\dot{V} = [(S - S_e) + (I - I_e) + (R - R_e)][(a - m)N - \phi N^2 - (a - \phi N)(1 - \rho)I - \alpha I] + \frac{(1 - \rho)(I - I_e)}{e\rho}\left[\frac{\beta S}{N} + e\rho(a - \phi N) - (\alpha + m + v)\right] + \frac{\alpha(R - R_e)}{v}[vI - (m + \delta)R]$$

This simplifies to

$$\dot{V} = [(S - S_e) + (I - I_e) + (R - R_e)][(a - m)N - \phi N^2 - (a - \phi N)(1 - \rho)I - \alpha I] + \frac{(1 - \rho)(I - I_e)}{e\rho}\left[\frac{\beta S}{N} + e\rho(a - \phi N) - (\alpha + m + v)\right] + \alpha(R - R_e)I - \frac{\alpha(m + \delta)}{v}(R - R_e)R$$

Substituting the following equalities:

$$(\alpha + m + v) = \beta\frac{S_e}{N_e} + e\rho(a - \phi N_e)$$

$$(m + \delta) = v\frac{I_e}{R_e}$$

$$(a - m) = \phi N_e + (a - \phi N)(1 - \rho)\frac{I_e}{N_e} + \alpha\frac{I_e}{N_e}$$

we have that

$$\dot{V} = [(S - S_e) + (I - I_e) + (R - R_e)]\left[\phi N_e N + (a - \phi N)N(1 - \rho)\frac{I_e}{N_e} + \alpha N\frac{I_e}{N_e} - \phi N^2 - (a - \phi N)(1 - \rho)I - \alpha I\right] + \frac{(1 - \rho)(I - I_e)}{e\rho}\left[\frac{\beta S}{N} + e\rho(a - \phi N) - \beta\frac{S_e}{N_e} - e\rho(a - \phi N_e)\right] + \alpha(R - R_e)I - \frac{\alpha I_e}{R_e}(R - R_e)R$$

which simplifies to

$$\dot{V} = (N-N_e)\left[-\phi N(N-N_e) + \frac{\alpha}{N_e}(I_e(N-N_e) - N_e(I-I_e)) + \frac{(1-\rho)}{N_e}(aI_e(N-N_e) - aN_e(I-I_e) + \phi NN_e(I-I_e)\right]$$
$$+ \frac{\beta(1-\rho)(I-I_e)}{e\rho NN_e}(N_e(S-S_e) - S_e(N-N_e)) - (1-\rho)\phi(I-I_e)(N-N_e) + \alpha(R-R_e)(I-I_e) - \alpha\frac{I_e}{R_e}(R-R_e)^2$$

Further simplifications using the equality, $(N-N_e) = (S-S_e) + (I-I_e) + (R-R_e)$ yielded that

$$\dot{V} = -(N-N_e)^2\left[\phi N - \frac{I_e}{N_e}(\alpha + a(1-\rho))\right] - (N-N_e)(I-I_e)\left[\alpha + (1-\rho)(a-\phi N) + (1-\rho) + \frac{\beta(1-\rho)S_e}{e\rho NN_e} - \frac{\beta(1-\rho)}{e\rho N}\right]$$
$$- \alpha\frac{I_e}{R_e}(R-R_e)^2 - (I-I_e)^2\frac{\beta(1-\rho)}{e\rho N} - (I-I_e)(R-R_e)\left[\frac{\beta(1-\rho)}{e\rho N} - \alpha\right]$$

$\dot{V} = 0$ iff $\frac{\phi NN_e}{I_e} > (\alpha + a(1-\rho))$, $\alpha + (1-\rho)a > (1-\rho)\phi N + \frac{\beta(1-\rho)}{e\rho N}$ and $\frac{\beta(1-\rho)}{e\rho N} > \alpha$. Combining these inequalities and substituting the expression for I_e led to the conclusion that $R_0 \geq 1$. We also noted that $\dot{V} = 0$ iff $S = S_e$, $I = I_e$, and $R = R_e$.

Therefore, the largest compact invariant set in $\{(S,I,R) \in \Omega : \dot{S}_e = 0\}$ is the singleton $\{E_e\}$, where E_e is the endemic equilibrium. It thus follows from the Lyapunov–Lasalle theorem [14] that E_e is globally asymptotically stable in Ω, and so every trajectory of System (1) approaches the endemic equilibrium for $R_0 \geq 1$. E_e is the unique steady state for System (1) when $R_0 \geq 1$. □

4. Numerical simulations

Numerical simulations were performed using the deSolve package in R [16](Appendix B) to illustrate some of the qualitative analytical findings.

4.1. Parameter values

The parameter values used for the simulations were obtained from published reports and articles on bison in natural parks such as those of Dobson [4]. For example, the calving rate was found to range between 0.42 and 0.82 [4, 17, 18]. The density-dependent reduction in host births (ϕ) was determined by assuming that the bison population may equilibrate at the carrying capacity of 4500 heads [4]. Brucellosis is not known to significantly increase the mortality in cows. However, because this model assumed that the infectious calves move directly into the infectious compartment (I), this compartment was associated with a low infection-related mortality rate (α) following death of infectious calves. The natural mortality rate was defined as the reciprocal of the life span of a bison determined to be between 15 and 25 years [4, 11]. Once infected, bison may stay infectious throughout their life span. However, they were assumed to contribute significantly to the transmission dynamics only during the first 2 years following infection [4]. For all other parameter values, possible values were presented in Table II.

4.2. Simulation of the infection-free and endemic steady states

Figure 2(a) and 2(b) demonstrate the convergence of the solution profile to the infection free rest point. The estimated basic reproduction number for these settings was less than unity, that is, $R_0 = 0.12$ and $R_0 = 0.95$, respectively. The plots indicated that an increase in the basic reproduction number from 0.12 to 0.95 had the effect of slightly increasing the time at which the infectious population reaches zero. In addition, after varying the initial values further away from the infection free equilibrium, the solutions still converged to the infection free equilibrium supporting our proposition of global stability (Figure 3(a) and 3(b)). Endemicity is depicted in Figure 4(a) and 4(b) with values of R_0 being 3.3 and 10.7, respectively. In this case, an increase in the basic reproduction number had the significant

Table II. Suggested parameter values for System (1).

Parameter	Value	Source
ϕ	0.00004	[4]
ρ	0.5	[4]
α	0.05	[4]
β	0.05–10	[4]
δ	0.2	[4]
e	0.9	[4]
v	0.5	[4]
m	0.04–0.07	[4, 11]
a	0.42–0.82	[4, 17, 18]

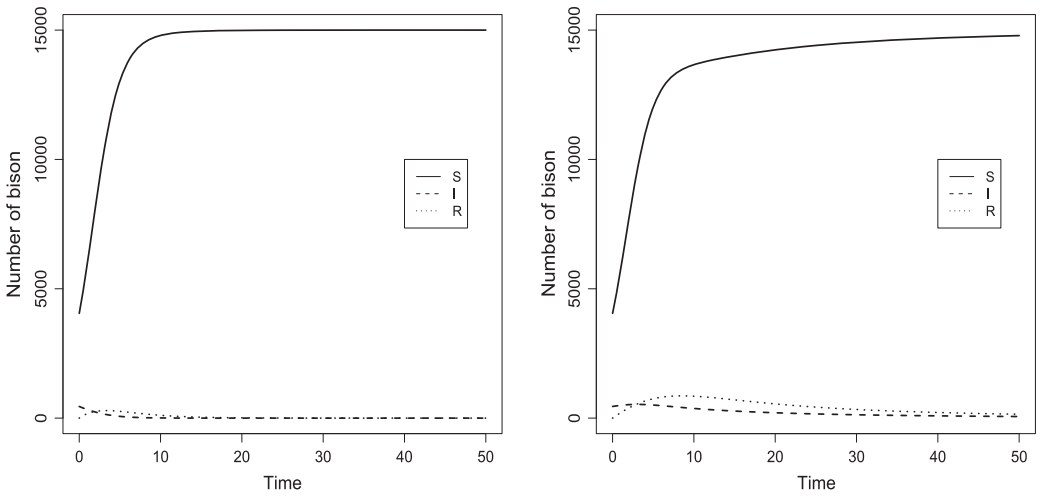

(a) $\beta = 0.05$, and $R_0 = 0.12$ (b) $\beta = 0.50$, and $R_0 = 0.95$

Figure 2. Numerical simulation of the time evolution of the infection free steady state. The parameters used are described in Table II. The initial values were: $(S_0, I_0, R_0) = (4050, 450, 0)$.

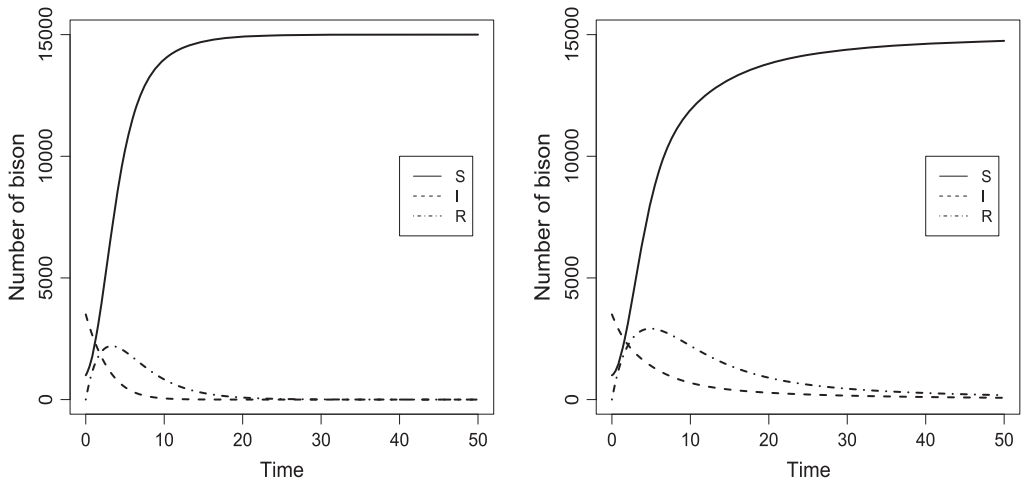

(a) $\beta = 0.05$, and $R_0 = 0.12$ (b) $\beta = 0.50$, and $R_0 = 0.95$

Figure 3. Numerical simulation of the time evolution of the infection free steady state. The parameters used are as described in Table II. The initial values were $(S_0, I_0, R_0) = (1000, 3500, 0)$.

effect of reducing the number of susceptible bison and increasing the number of infectious bison. It was noted that no matter which starting values were chosen for (S_0, I_0, R_0) (with $S_0 > 0, I_0 > 0$, and $R_0 \geq 0$), the trajectories converged to the endemic equilibrium (Figure 5(a) and 5(b)).

4.3. Global sensitivity analysis

A global sensitivity analysis was conducted to determine the influence of uncertainties in parameter values on the variability of the expected number of infectious bison ($\hat{I}$) at given time points. There are several measures that can be used to determine global sensitivity of parameters; those that are based on sampling and those that are based on decomposition of variances. The most popular sampling-based measure is the partial ranked correlation coefficient (PRCC), whereas the most commonly used variance-based methods are the Sobol first order and total effect indices [10, 19]. The PRCC is a robust sensitivity measure for nonlinear but monotonic relationships between model parameters and model outputs and can be used to determine the influence of an increase or decrease in parameter values linearly discounting the effects of the uncertainty over the rest of the parameters of the model [20–23]. It therefore provides information that can be used to inform decision makers on which parameters to target in order to achieve desired levels of prevention and control. On the other hand, the variance-based Sobol indices indicate parameters whose uncertainty influences the variability of the expected number of infectious bison ($\hat{I}$). They can therefore indicate parameter values for which the level of uncertainty has to be decreased through field studies or tailored experiments in order to reduce the uncertainties in output parameters [10]. The Sobol first-order index gives a measure of the direct effect of a model parameter on the variation in $\hat{I}$, whereas the total-order index

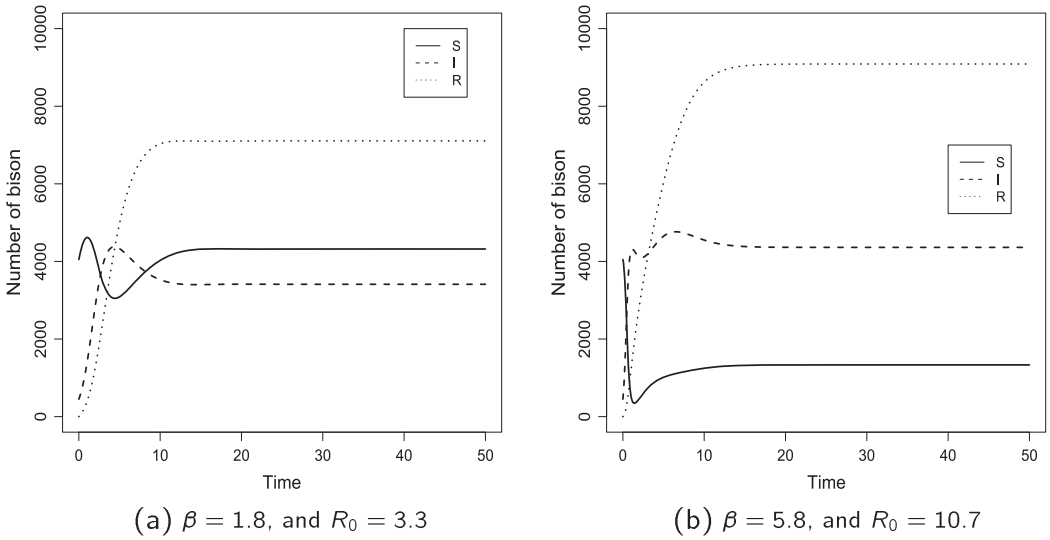

Figure 4. Numerical simulation of the time evolution of the endemic steady state $a = 0.64$, $m = 0.04$, $\phi = 0.00004$, $v = 0.5$, $\rho = 0.5$, $e = 0.9$, $\delta = 0.2$, and $\alpha = 0.005$. The initial values were (S_0, I_0, R_0)=(4050,450,0).

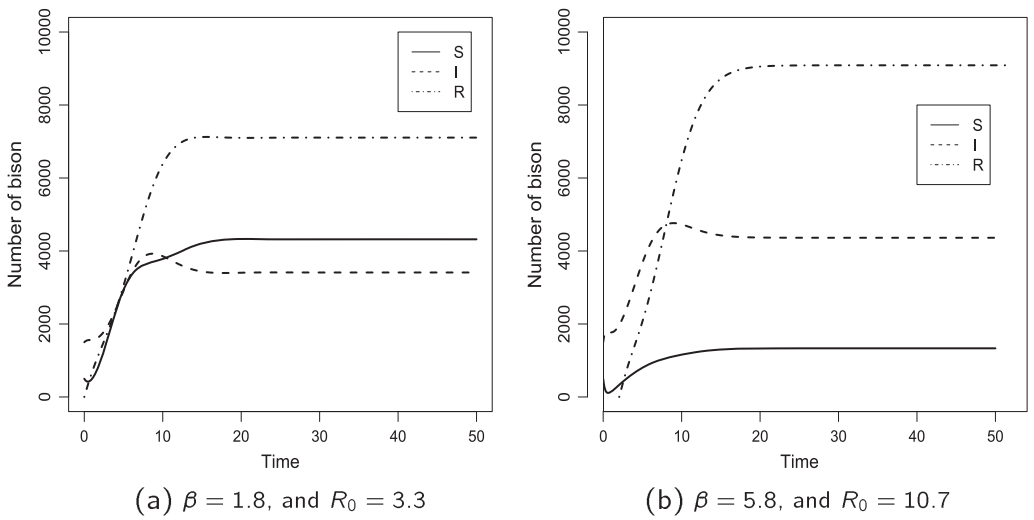

Figure 5. Numerical simulation of the time evolution of the endemic steady state $a = 0.64$, $m = 0.04$, $\phi = 0.00004$, $v = 0.5$, $\rho = 0.5$, $e = 0.9$, $\delta = 0.2$, and $\alpha = 0.005$. The initial values were (S_0, I_0, R_0)=(500,1500,0).

describes the share of the output variation that is related to each input factor. It includes the direct effect as well as interactions among the other parameters [24]. As suggested by Marino et al. 2008 [10], because the two methods measure different aspects of the model, the most optimal strategy to achieving a complete and informative sensitivity analysis is to estimate both indices. The distributions of the parameters were based on the Triangular distribution. The mode of the Triangular distribution in each setting was the value of the parameter (Table II), and the maximum and minimum values were arbitrarily chosen.

The Sobol indices were consistently high for the rate of loss of resistance, δ and the recovery rate, v for the three time points considered indicating that these parameters were very sensitive to variabilities in the expected number of infectious bison. All the other parameters had moderate (for a) to relatively minor impact on the variability of the expected number of infectious bison (Table III). The Sobol indices appeared to vary along the three times point. The Sobol first-order indices for all parameters gave a sum of 1.192 meaning that the output does not seem to be affected by interactions among the parameters. The total effect indices for δ and v were again consistently higher compared to those of the other parameters.

The parameters a, ϕ, δ, and v were found to consistently exhibit high correlations across the three time points, whereas β and m were found to exhibit moderate correlations with $\hat{I}$. An increase in the values of ϕ, v, or m will lead to a corresponding decrease in the estimated number of infectious bison $(\hat{I})$. On the other hand, decreasing the value of δ, β, or a will lead to a corresponding decrease in the value of $\hat{I}$ (Table IV).

Table III. First-order and total-effect sensitivity indices for expected number of infectious bison $(\hat{I})$ at three time points ($t = 10, 25$, and 50).

	First order				Total effects		
Parameter	$t = 10$	$t = 25$	$t = 50$	Parameter	$t = 10$	$t = 25$	$t = 50$
β	0.037*	0.024	0.026	β	−0.001	0.024	0.003
a	0.209*	0.215*	0.141*	a	0.079	0.029	0.078
m	0.011	0.031	0.132*	m	0.010	0.044	0.119*
ϕ	0.217*	0.070	0.037	ϕ	0.019	0.061	0.129*
v	0.408*	0.412*	0.303*	v	0.441*	0.309*	0.327*
ρ	0.009*	0.005*	0.007*	ρ	−0.008*	−0.005*	−0.007*
δ	0.290*	0.505*	0.278*	δ	0.249*	0.327*	0.452*
α	0.007*	0.007*	0.007*	α	−0.007*	−0.006*	−0.007*
e	0.008*	0.007*	0.006*	e	−0.008*	−0.007*	−0.006*

t, time;
* Significant at 5% level; the negative values for these indices indicate that the analytical sensitivity indices are close to zero (i.e., for unimportant factors)[19].

Table IV. Partial rank correlation coefficients (PRCCs) between each model parameter and the estimated number of infectious bison $(\hat{I})$ at three time points ($t = 10, 25$, and 50) using 11000 replications.

Parameter	$t = 10$	$t = 25$	$t = 50$
β	0.529*	0.488*	0.450*
a	0.842*	0.784*	0.711*
b	−0.288*	−0.578*	−0.756*
ϕ	−0.788*	−0.699*	−0.639*
v	−0.943*	−0.915*	−0.881*
ρ	−0.038*	−0.013*	0.035*
δ	0.919*	0.935*	0.901 *
α	−0.008	−0.0138	−0.016
e	0.021*	−0.017	−0.010

t,time;
*Significant at the 5% level.

4.4. Control of bovine brucellosis in bison

The control of diseases in wild life is very expensive, and therefore, the evaluation of control strategies based on dynamic models is the key to eradicating the infection. Culling and vaccination coupled with good herd management are common methods that have been used to reduce the size of susceptible animals in a population to levels below the threshold for transmission [4, 25]. The choice of which control strategy is most effective depending on the disease and its epidemiological characteristics. For most directly transmissible diseases, culling or vaccination alone has been shown to be more appropriate, whereas for others, a combination of both methods is the most optimal strategy [25]. For our model, culling is related with mortality rate, birth rate, density-dependent reduction in birth rate, loss of resistance, and the transmission coefficient whereas vaccination will directly influence the recovery rate and the transmission rate.

4.4.1. Culling. Even though the simplest control measure is that of regularly culling host animals, it has been the subject of much recent debates. If a proportion γ of infectious bisons is culled each year, replacing m with $m + \gamma$ of System (1) will yield the following modified threshold for the eradication or persistence of disease [26]:

$$R_c = \frac{\beta + e\rho m}{(\alpha + m + \gamma + v)}$$

For an infection free herd, $R_c < 1$ or $\frac{\beta + e\rho a}{(\alpha + m + \gamma + v)} < 1$ from which it follows that the yearly culling rate that will eliminate the infection $\gamma_c = (\beta + e\rho m) - (\alpha + m + v)$.

The results of the numerical simulations in Figure 6 reflect the effects of culling on the number of bison in each disease state in the population. The culling threshold for eradication of the infectious bison population was 1.3 for the given set of parameters. Below this value, the infection persists (Figure 6(a)), whereas above this value, the infection vanishes (Figure 6(b)).

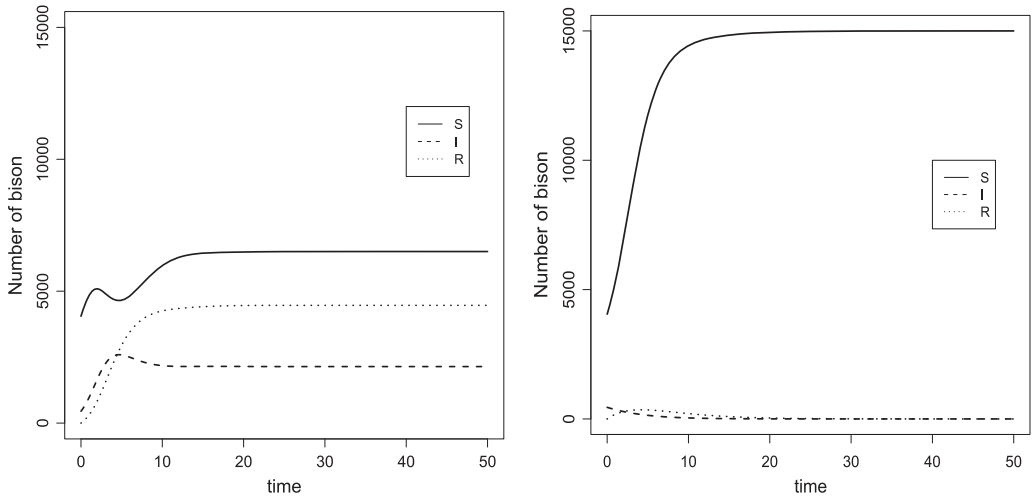

Figure 6. Numerical simulations of the effect of culling. Model parameter values are $a = 0.64$, $m = 0.04$, $\phi = 0.00004$, $v = 0.5$, $\rho = 0.5$, $e = 0.9$, $\delta = 0.2$, and $\alpha = 0.005$. The initial values were (S_0, I_0, R_0)=(4050,450,0).

4.4.2. Vaccination. The RB51 vaccine has been evaluated for its potential use in the eradication of brucellosis in bison herds and found to offer protection against abortion and vertical transmission [27, 28]. Because this vaccine has not been fully implemented in the YNP, its effects are evaluated based on numerical simulations. Suppose that a proportion, p, of the susceptible bison population is vaccinated yearly with a vaccine that offers only temporal immunity. In addition, let's assume that the vaccine is given to a proportion q of the newborns. Defining a new class to represent the vaccinated sub-population, U, it follows that a fraction of the newborns, q, will move into the vaccinated class, whereas the remaining proportion $(1 - q)$ will stay in the susceptible class. In addition, a portion p of the susceptible population will move into the vaccination class per year. Finally, after a period $1/\delta_2$, vaccinated bison lose their immunity to become susceptible again. The vaccine is assumed to be 100% effective and to have no effect on the infectious bison. A modified version of System 1 that incorporates the vaccinated fraction of the population is given as follows [29, 30]:

$$\begin{aligned}
\frac{dS(t)}{dt} &= (1-q)(a-\phi N_u)[S+U+R+I\rho(1-e)] - mS + \delta R - \beta\frac{I}{N_u}S + \delta_2 U - pS \\
\frac{dI(t)}{dt} &= \beta\frac{I}{N_u}S + e\rho(a-\phi N_u)I - (\alpha+m+v)I \\
\frac{dR(t)}{dt} &= vI - (m+\delta)R \\
\frac{dU(t)}{dt} &= q(a-\phi N_u)[S+U+R+I\rho(1-e)] + pS - (m+\delta_2)U \\
\frac{dN_u}{dt} &= (a-\phi N_u)N_u - (a-\phi N_u)(1-\rho)I - \alpha I - mN_u \\
S(0) &> 0,\ I(0) \geq 0,\ R(0) \geq 0,\ U(0) \geq 0 \text{ and } N_u(0) > 0
\end{aligned} \tag{2}$$

where q and p are additional constants and now $N_u = S+I+R+U$. The basic reproduction number under vaccination was qualitatively derived using the Next Generation matrix approach [31].

$$\begin{aligned}
\frac{dI(t)}{dt} &= \beta\frac{I}{N_u}S + e\rho(a-\phi N_u)I - (\alpha+m+v)I \\
\frac{dU(t)}{dt} &= q(a-\phi N_u)[S+U+R+I\rho(1-e)] + pS - (m+\delta_2)U
\end{aligned} \tag{3}$$

This approach starts out by considering the differential equations for the two infected compartments I and V (System (3)). From these equations, entries for the two matrices $\mathcal{F}$ and $\mathcal{V}$ were derived. The entries of $\mathcal{F}$ represent the rate of acquisition of new infections into the two compartments and those of $\mathcal{V}$, the transfer rate of individuals in and out of the compartments. $\mathcal{F}$ and $\mathcal{V}$ were obtained as follows:

$$\mathcal{F} = \begin{pmatrix} \beta\frac{I}{N_u}S + e\rho(a-\phi N_u)I \\ q(a-\phi N_u)(I\rho(1-e) \end{pmatrix} \text{ and } \mathcal{V} = \begin{pmatrix} (\alpha+m+v)I \\ (m+\delta_2)U - q(a-\phi N_u)[S+U+R] - pS \end{pmatrix}$$

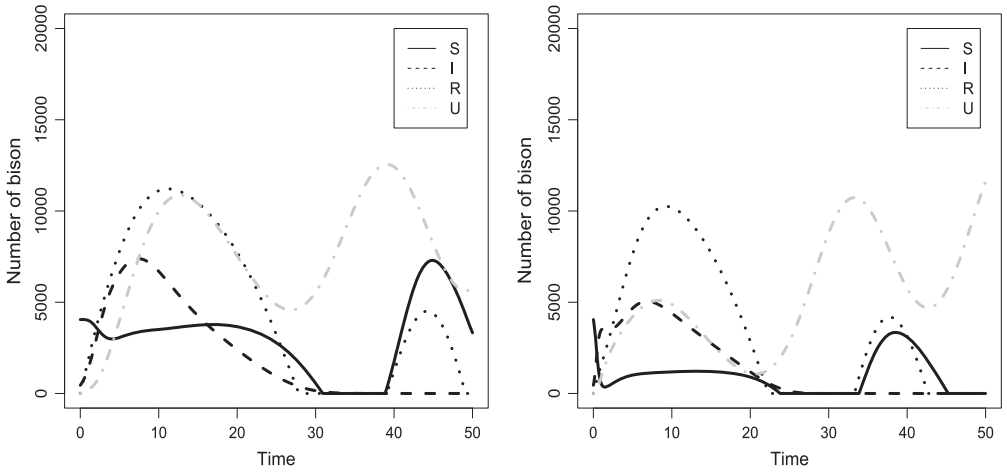

(a) p=0.13/year, q=0.25, β=1.8 (b) p=0.25/year, q=0.40, β=5.8

Figure 7. Numerical simulations of the effects of vaccination. Model parameter values are $a = 0.64$, $m = 0.04$, $\phi = 0.00004$, $v = 0.5$, $\rho = 0.5$, $e = 0.9$, $delta = 0.2$, $\delta_2 = 0.005$, and $\alpha = 0.005$.

The derivatives of $\mathcal{F}$ and $\mathcal{V}$ denoted by **F** and **V**, respectively, evaluated at the infection free steady state E_{v0} yields

$$\mathbf{F} = \begin{pmatrix} \frac{\beta(\delta+m(1-q))}{(\delta+m+p)} + e\rho m & 0 \\ pq(1-e)m & 0 \end{pmatrix} \text{ and } \mathbf{V} = \begin{pmatrix} (\alpha+m+v) & 0 \\ q(a-m) & (m+\delta_2)+q(a-2m) \end{pmatrix}$$

The inverse of **V** is given by

$$\mathbf{V}^{-1} = \frac{1}{(\alpha+m+v)(m+\delta_2+q(a-2m))} \begin{pmatrix} (m+\delta_2)+q(a-2m) & 0 \\ -q(a-m) & (\alpha+m+v) \end{pmatrix}$$

The next generation matrix is calculated as follows:

$$\mathbf{FV}^{-1} = \begin{pmatrix} \frac{\beta(\delta+m(1-q))}{(\delta+m+p)(\alpha+m+v)} + \frac{e\rho m}{(\alpha+m+v)} & 0 \\ \frac{pq(1-e)m}{(\alpha+m+v)} & 0 \end{pmatrix}$$

The vaccination reproduction number R_v is given by the spectral radius of the next generation matrix, that is, $R_v = \rho(\mathbf{FV}^{-1})$. It follows that

$$R_v = \frac{\beta(\delta+m(1-q))}{(\delta+m+p)(\alpha+m+v)} - \frac{\beta}{(\alpha+m+v)} + \frac{\beta+e\rho m}{(\alpha+m+v)} = R_0 - \frac{\beta(p+mq)}{(\delta+m+p)(\alpha+m+v)}$$

It can be clearly seen from this expression that R_v factored out into R_0 and a component depended on the vaccination promotion.

An alternative method for deriving the basic reproduction number was through linearization of System 2 around the infection free steady state (Appendix A).

Numerical simulations illustrating the effects of vaccination are shown on Figure 7. Comparing the simulation results with those of the model without vaccination (Figure 4), it was observed that vaccinating the susceptible bison at a yearly rate of 0.13 and 25% of the newborns each year, the infection vanished from the herd after 30 years. The vaccination reproductive number in this case was less than unity ($R_v = 3.3 - 2.64 = 0.66$)(7(a)). Increasing the value of the value of the transmission rate parameter from 1.8 to 5.8 and also the vaccinated fractions from 0.13 and 0.25 to 0.18 and 0.42, respectively, caused the infection to persist for a longer period (up to 45 years). The vaccination reproductive number was less than unity ($R_v = 10.7 - 9.74 = 0.96$)(7(b)).

5. Discussion

In this study, a mathematical model previously proposed for studying the epidemiology of brucellosis was qualitatively and quantitatively examined. Threshold parameters were derived for the system and its variants. Using numerical simulations, it was shown that for all systems, the infection vanished when the basic reproduction number was below unity and persisted otherwise. However, for the model with vaccination, the basic reproduction numbers were smaller even for very high magnitudes of the transmission rate parameter as compared with those of the simple model without vaccination.

The results of the global sensitivity analysis using the Sobol indices indicated that the rate of loss of resistance and the recovery rate caused most of the variability in the expected number of infectious bison for the three different time points evaluated. An increase in the precision of the estimates of these parameters will lead to more accurate estimations of the expected outputs of the system. Epidemiological studies are therefore needed to estimate these parameters under field conditions. On the other hand, the PRCCs indicated that the density-dependent reduction in birth rate, ϕ, the loss of resistance, δ, the recovery rate, v, and the calving rate, a, exhibited very high correlations ($|PRCCs| > 0.5$) with $\hat{I}$, the estimated number of infectious bison. The rate of loss of resistance, the birth rate, and the transmission coefficient can be decreased by the application of control policies such as vaccination or the removal of bison that have recovered from the infection. This way, fewer recovered animals will move to the susceptible class. The mortality rate can be increased by culling susceptible and infectious bison. This has the effect of reducing the total population size to levels too low to sustain the infection.

The transmission of brucellosis among bison in a herd results from the large amount of bacteria shed in the environment following an abortion or parturition. However, most models for brucellosis have considered a direct transmission route between susceptible and infectious animals [32, 33]. The parameter, β, which quantified the direct transmission between infectious and susceptible bison appeared to have a moderate correlation (0.5 on average) with the estimated number of infectious bison. This is an indication that the assumption of a direct transmission route for brucellosis needs to be re-evaluated. In addition, this may be an indication that modeling the transmission as frequency dependence needs to be re-evaluated as well. This comes as a result of the indirect transmission nature of brucellosis following the discharge of large amounts of bacteria in tissues after calving or abortion. A larger number of infectious bison within a fixed area will mean that more bacteria will be shed into the environment thus increasing the probability of picking up bacteria and getting infected. However, it has been demonstrated by Dobson [4] that frequency-dependent transmission is to be preferred as it produced levels of prevalence that closely resembled those observed in serological surveys. A study which couples both the direct and indirect transmission routes for brucellosis and which compares frequency and density-dependent transmissions is in progress.

Our model was based on several simplifying assumptions: the infectious animal population was not partitioned into abortives and non-abortives. However, this distinction is important because time to abortion and time to full term birth are different [32]. It was also assumed that calves are immediately susceptible to the disease and can get infected and move into the infectious class. However, it is not clear if all infectious bison calves end up as infected female adult bison or if the infection causes sterility. For the sake of clarity, some other authors have assumed that calves attain sexual maturity before being considered susceptible [3]. The investigation of these assumptions is the topic of work in progress. Most recently, Aïnseba et al. (2009) proposed a model for ovine brucellosis, which incorporated both direct and indirect transmission mechanisms. However, the model did not distinguish between abortive and non-abortive infectious sheep and newborns that were considered to be directly susceptible [34].

Two main control strategies, culling and vaccination, were investigated for their role in the eradication of brucellosis in bison herds. It was observed that culling infectious bison at the hypothetical yearly rate of 1.5 led to the eradication of the infection with the susceptible population growing to the carrying capacity of the YNP. Because the sensitivity analysis indicated that direct transmission plays a less significant role, on the dynamic of bison, indirect transmission following shedding of bacteria in the environment could be the main transmission route. A demonstration of the importance of indirect transmission will mean that culling has no effect on the transmission of brucellosis in the face of indirect transmission because even if infected bison are culled or removed from the herd infectious units may stay in the environment. Vaccination was observed to decrease the basic reproduction number by a quantity that depended on the vaccination fraction of susceptible bison and newborns. Because test and slaughter is very costly and hence an infeasible option for brucellosis in bison herds, culling of bison that attempts to leave the park combined with other control measures such as vaccination and good herd management could be a more plausible control option.

The transmission dynamics in this study were of a general nature with limited references to the YNP. The model can be easily adapted to any natural park with free ranging bison. To effectively guide public health policy and public health decision making, the model and parameter values would need to be validated using data from National parks.

Acknowledgements

This work was supported by the Belgian Cooperation in the framework of the Institutional Collaboration between the Institute of Tropical Medicine in Antwerp, Belgium and the Centro Internacional de Zoonosis in Quito, Ecuador.

References

1. Anonymous. Brucellosis in humans and animals 2006. *WHO Library Cataloguing-in-Publication Data*.
2. Pappas G, Akritidis N, Bosilkovski M, Tsianos E. Brucellosis. *New England Journal of Medicine* 2005; **352**:2325–2336.
3. England T, Kelly L, Jones RD, MacMillan A, Wooldridge M. A simulation model of brucellosis spread in British cattle under several testing regimes. *Preventive Veterinary Medicine* 2004; **63**:63–73.
4. Dobson A, Meagher M. The population dynamics of Brucellosis in the Yellowstone National Park. *Ecology* 1996; **77**:1026–1036.
5. Kilpatrick AM, Gillin CM, Daszak P. Wildlife-livestock conflict: the risk of pathogen transmission from bison to cattle outside Yellowstone National Park. *Journal of Applied Ecology* 2009; **46**:476–485.
6. Rhyan JC, Gidlewski T, Roffe TJ, Aune K, Philo LM, Ewalt DR. Pathology of brucellosis in bison from Yellowstone National Park. *Journal of Wildlife Diseases* 2001; **37**:101–109.

7. Mohler JR, *Abortion disease. in Annual report*, Technical Report, Bureau of animal industry, Department of Agriculture, Government Printing Office, Washington, D.C., 1917. Pages 105–106.
8. Davis PH, Elzer DS. Brucella vaccines in wildlife. *Veterinary Microbiology* 2002; **90**:533–544.
9. Plumb GE, Whitea P, Coughenourb MB, Wallena RL. Carrying capacity, migration, and dispersal in Yellowstone bison. *Biological Conservation* 2009; **142**:2377–2387.
10. Marino S, Hogue IB, Ra CJ, Kirschner DE. A methodology for performing global uncertainty and sensitivity analysis in systems biology. *Journal Theoretical Biology* 2008; **254**:178–196.
11. Miller KL, *Planning for bison grazing on native rangeland*, Technical Report, USDA -Natural Resources Conservation Service, 2002.
12. Esteva L, Vargas C. Analysis of a dengue disease transmission model. *Mathematical Biosciences* 1998; **150**:131–151.
13. Hethcote HW. The mathematics of infectious diseases. *Society for Industrial and Applied Mathematics* 2000; **42**:599–653.
14. LaSalle JP. *The Stability of Dynamical Systems*. Society for Industrial and Applied Mathematics: Philadelphia, 1976.
15. Edelstein-Keshet L. *Mathematical Models in Biology*. Society for Industrial and Applied Mathematics: Philadelphia, 2005.
16. Team RDC. *R: A Language and Environment for Statistical Computing* 2.14.1 edn. R Foundation for Statistical Computing: Vienna, Austria, 2012. ISBN 3-900051-07-0.
17. Fuller JA, Garrott RA, White PJ, Aune KE, Roffe TJ, Rhyan JC. Reproduction and Survival of Yellowstone Bison. *Journal of Wildlife Management* 2007; **71**:2365–2372.
18. Treanor JJ, Johnson JS, Wallen RL, Cilles S, Crowley PH, Cox JJ, Maehr DS, White PJ, Plumb GE. Vaccination strategies for managing brucellosis in Yellowstone bison. *Vaccine* 2010; **28**(Suppl 5):F64–F72.
19. Saltelli A. Sensitivity analysis for importance assessment. *Risk Analysis* 2002; **22**:579–590.
20. Blower SM, Dowlatabadi H. Sensitivity and uncertainty analysis of complex models of disease transmission: an HIV model as an example. *International Statistical Review* 1994; **62**:229–243.
21. Ivanek R, Snary EL, Cook AJC, Gröhn YT. A mathematical model for the transmission of Salmonella Typhimurium within a grower-finisher pig herd in Great Britain. *Journal of Food Protection* 2004; **67**:2403–2409.
22. Rong L, Feng Z, Perelson AS. Emergence of HIV-1 drug resistance during antiretroviral treatment. *Bulletin of Mathematical Biology* 2007; **69**: 2027–2060.
23. Sanchez MA, Blower AM, Uncertainty. Uncertainty and sensitivity analysis of complex models of disease transmission: an HIV model as an example. *American Journal of Epidemioly* 1997; **145**:1127–1137.
24. Elleithy K. *Innovations and Advanced Techniques in Systems, Computing Sciences and Software Engineering*. Springer: New York, 2008.
25. Wang X, Lou J. Two dynamic models about rabies between dogs and human. *Journal of Biological Systems* 2008; **16**:519–529.
26. Roberts MG. The dynamics and control of bovine tuberculosis in possums. *IMA Journal of Mathematics Applied in Medicine and Biology* 1992; **9**:19–28.
27. Olsen SC, Holland SD. Safety of revaccination of pregnant bison with Brucella abortus strain RB51. *Journal of Wildlife Diseases* 2003; **39**:824–829.
28. Olsen SC, Boyle SM, Schurig GG, Sriranganathan NN. Efficacy of dart or booster vaccination with strain RB51 in protecting bison against experimental Brucella abortus challenge. *Clinical Vaccine and Immunology* 2009; **16**:535–540.
29. Ma S, Xia Y. *Mathematical Understanding of Infectious Disease Dynamics*. World Scientific Publishing: Singapore, 2009.
30. Takeuchi Y, Iwasa Y, Sato K. *Mathematics for Life Science and Medicine*. Springer Berlin: Heidelberg New York, 2007.
31. Van den Driessche P, Watmough J. Reproduction numbers and sub-threshold endemic equilibria for compartmental models of disease transmission. *Mathematical Biosciences* 2002; **180**:29–48.
32. Gonzlez-Guzmn J, Naulin R. Analysis of a model of bovine brucellosis using singular perturbations. *Journal of Mathematical Biology* 1994; **33**: 211–223.
33. Zinsstag J, Roth F, Orkhon D, Chimed-Ochir G, Nansalmaa M, Kolar J, Vounatsou P. A model of animal-human brucellosis transmission in Mongolia. *Preventive Veterinary Medicine* 2005; **69**:77–95.
34. Aïnseba B, Benosman C, Magal P. A model for ovine brucellosis incorporating direct and indirect transmission. *Journal of Biological Dynamics* 2009; **4**:2–11.